

HRCT features distinguishing pre-invasive from invasive pulmonary adenocarcinomas appearing as ground-glass nodules

Yu Zhang¹ · Yan Shen² · Jin Wei Qiang¹ · Jian Ding Ye² · Jie Zhang³ · Rui Ying Zhao³

Received: 31 March 2015 / Revised: 9 November 2015 / Accepted: 23 November 2015 / Published online: 11 December 2015
© European Society of Radiology 2015

Abstract

Objective To investigate the high-resolution computed tomography (HRCT) features that distinguish lung adenocarcinomas in situ (AISs) and minimally invasive adenocarcinomas (MIAs) from invasive adenocarcinomas (IACs) appearing as ground-glass nodules (GGNs), and to select candidates for sublobar resection.

Methods Two hundred and twenty-nine patients with 237 GGNs of less than 2 cm (139 AIS-MIA nodules and 98 IAC nodules) confirmed by surgery and pathology were retrospectively reviewed. The HRCT features of the AIS-MIAs and IACs were analysed and compared. Receiver operating characteristic (ROC) analyses were conducted to determine the cutoff values for the qualitative variables and their diagnostic performances.

Results Significant differences were found in the density, nodule and solid component diameters, CT values of the ground-glass and solid components, lobulated shape, spiculated margin, abnormal pulmonary vein and artery, air bronchogram, and pleural indentation of the GGNs between the two groups. Multivariate and ROC analyses revealed that larger diameter of nodules (≥ 12.2 mm) and solid components (≥ 6.7 mm), and

higher CT values of the solid components (≥ -192 HU) in the GGNs with air bronchogram were significantly associated with IACs.

Conclusions HRCT can identify distinguishing morphological features between AIS-MIAs and IACs, and is helpful for selecting candidates for sublobar resection.

Key Points

- IACs appearing as GGNs were often ≥ 12.2 mm in diameter.
- IACs were often ≥ 6.7 mm in solid component diameter.
- The solid components of the IACs often exhibited ≥ -192 HU.
- IACs exhibited air bronchogram more frequently than AIS-MIAs.

Keywords Lung neoplasms · Ground-glass nodule · Adenocarcinoma in situ · Adenocarcinoma · Invasive · Tomography · X-ray computed

Abbreviations

AIS	Adenocarcinoma in situ
MIA	Minimally invasive adenocarcinoma
IAC	Invasive adenocarcinoma
AAH	Atypical adenomatous hyperplasia
GGN	Ground-glass nodule
PGGN	Pure ground-glass nodule
MGGN	Mixed ground-glass nodule
HRCT	High-resolution computed tomography

Introduction

Ground-glass nodules (GGNs) are becoming a major concern due to their possible association with lung adenocarcinomas [1]. In a new multidisciplinary classification of lung adenocarcinomas that was introduced in 2011 [2], the terms

✉ Jin Wei Qiang
dr.jinweiqiang@163.com

✉ Jian Ding Ye
yejianding@126.com

¹ Department of Radiology, Jinshan Hospital & Shanghai Medical College, Fudan University, Shanghai 201508, China

² Department of Radiology, Chest Hospital, Shanghai Jiaotong University, Shanghai 200030, China

³ Department of Pathology, Chest Hospital, Shanghai Jiaotong University, Shanghai 200030, China

Table 1 Morphological features of the GGNs in the AIS-MIA and IAC groups on HRCT

Features	AIS-MIAs (n = 139)	IACs (n = 98)	P Value
Density (PGGN/MGGN)	81/58	7/91	0.000 [§]
Diameter of nodule (mm)	11.1 ± 3.4	15.2 ± 3.1	0.000 [†]
Diameter of solid component (mm)	6.1 ± 3.2	10.3 ± 4.1	0.000 [†]
CT value of ground glass component (HU)	-545.8 ± 123.6	-395.7 ± 185.2	0.000 [†]
CT value of solid component (HU)	-230.5 ± 111.3	-130.3 ± 109.3	0.000 [†]
Lobulated shape	21 (15.1 %)	45 (45.9 %)	0.000 [§]
Spiculated margin	4 (2.9 %)	11 (11.2 %)	0.009 [§]
Abnormal pulmonary vein	43 (30.9 %)	74 (75.5 %)	0.000 [§]
Abnormal pulmonary artery	21 (15.1 %)	58 (59.2 %)	0.000 [§]
Air bronchogram	47 (33.8 %)	76 (77.6 %)	0.000 [§]
Bubble lucency	9 (6.5 %)	11 (11.2 %)	0.195 [§]
Pleural indentation	22 (15.8 %)	38 (38.8 %)	0.000 [§]

GGN: ground-glass nodule; PGGN: pure GGN; MGGN: mixed GGN; AIS: adenocarcinoma in situ; MIA: minimally invasive adenocarcinoma; IAC: invasive adenocarcinoma

[†] Two-sample Wilcoxon rank-sum test

[§] Pearson χ^2 test

adenocarcinoma in situ (AIS) and minimally invasive adenocarcinoma (MIA) were introduced due to the 100 % and near 100 % 5-year disease-free survivals, respectively, of these conditions following complete resection [2]. In contrast, the 5-year disease-free survival of invasive adenocarcinomas (IACs) of pathological stage IA is 74.6 % [3].

The introductions of AIS and MIA for pulmonary adenocarcinomas imply the possibility of sublobar resection involving anatomical segmentectomy and wedge excision for these lesions [4–6]. Recently, sublobar resection and lobectomy were shown to elicit comparable survival rates in stage IA lung cancer patients with nodules less than 2 cm [7, 8], and systematic lymph node dissection is not always required [9]. Thus, it is important to accurately discriminate AISs and MIAs from IACs prior to or during surgery, because lobectomy is required for IACs.

Several studies [2, 10, 11] have revealed that lung adenocarcinomas appearing as GGNs on high-resolution computed tomography (HRCT) also exhibit synchronous multiplicity (23 %–34 % or higher); therefore, patients with multiple

nodules require bilobectomy, lobectomy with wide wedge resection, multiple wide wedge resections or segmentectomies [4], underlining the need to preserve as much lung parenchyma as possible to maintain normal pulmonary function. Therefore, the purpose of our study was to investigate the HRCT features that distinguish AIS-MIAs from IACs amongst GGNs of less than 2 cm, and to define criteria for the selection of candidates for sublobar resection.

Materials and methods

Patients

The Institutional Review Board approved this retrospective study, and informed consent was waived. From April 2012 to April 2013, 229 consecutive patients with 237 GGNs < 2 cm were reviewed. All of the nodules underwent surgical resection and were pathologically confirmed to be AISs, MIAs or IACs (80 AISs, 59 MIAs, and 98 IACs). Among the

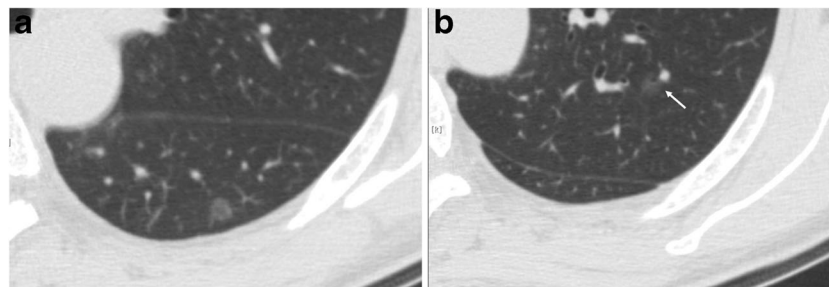


Fig. 1 A 57-year-old woman with multiple GGNs in the left lung. Axial HRCT image showing a 6.1-mm diameter GGN in the lower lobe with a CT value of -566 HU that was proven to be a AIS (a). Image of the upper

lung showing a 6.5-mm diameter GGN in the upper lobe with a bubble lucency and a CT value of -700 HU (white arrow); this nodule was not resected (b)

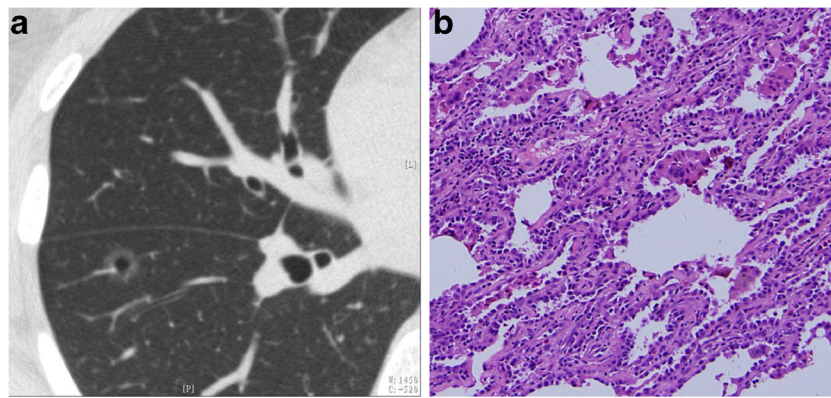


Fig. 2 A 34-year-old woman with a MIA in the right lower lobe of the lung. Axial HRCT image showing a 11.2-mm diameter oval PGGN with a bubble lucency and a CT value of -654 HU (a). Photomicrograph of the

resected specimen showing lepidic predominant lesion consisting of an invasive area of less than 5 mm in diameter with an acinar growth pattern [b, hematoxylin and eosin (H & E), ×100]

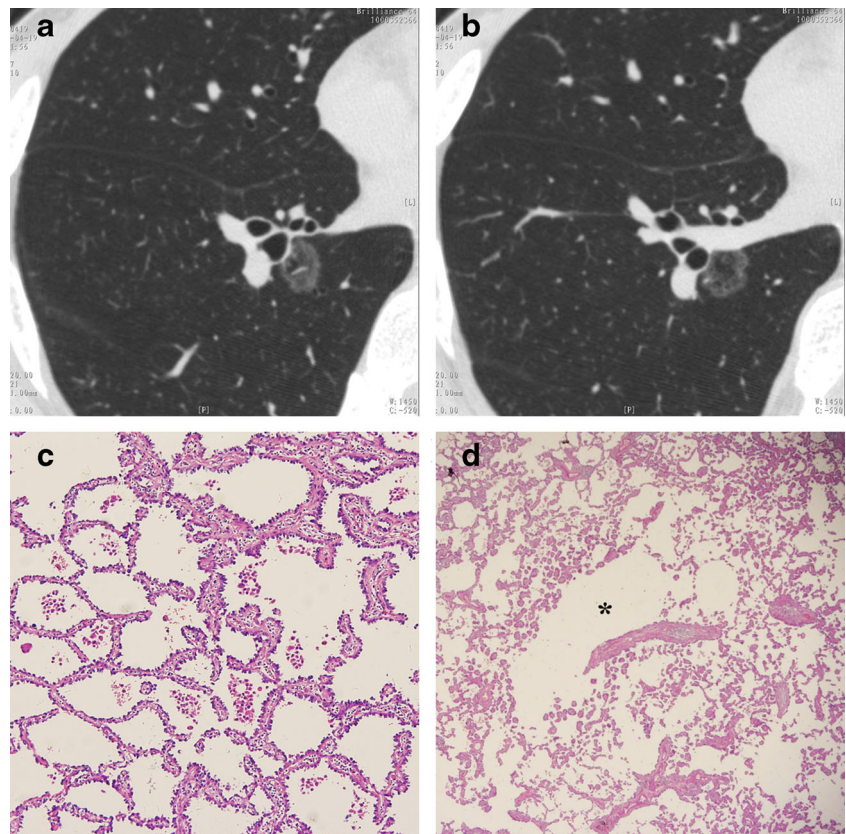
patients, 222 had single pulmonary nodules (128 AISs or MIAs and 94 IACs), and the remaining seven patients had multiple nodules (two patients had one MIA and one AIS, three patients had one IAC and one AIS, one patient had two AISs, and one patient had two AISs and one IAC). The patients ranged in age from 25 to 80 years (average 55.5 ± 9.9 years) and included 59 males and 170 females.

In the 229 enrolled patients, 77 (34 %) patients exhibited synchronous multiple pulmonary nodules on routine CT. Only 15 synchronous nodules in seven of the 77 patients met the inclusion criteria of this study. The remaining synchronous

nodules were not enrolled because they were AAHs or larger than 2 cm, or because the patient had not undergone a target HRCT scan.

Among the 128 enrolled patients with single AIS-MIA nodules and 94 enrolled patients with single IAC nodules, the lobectomy, segmentectomy, and wedge resection were performed in 98, 14, and 16 patients; and in 87, two, and five patients, respectively. Of the seven enrolled patients with multiple resected nodules, multiple nodules in the same lobe were observed in six patients, and these patients underwent lobectomies (five patients) or wedge resection (one patient), and the

Fig. 3 A 46-year-old man with a lepidic predominant IAC in the right lower lobe of the lung. Axial HRCT images (a, b) showing a 16.7-mm diameter lobulated PGGN with a bubble lucency and a CT value of -668 HU. Photomicrograph of the resected specimens showing a lepidic growth pattern with a slight papillary growth pattern (c, H & E, ×100) and non-lung architecture that correlated with the bubble lucency area (d, H & E, ×20) (asterisk)



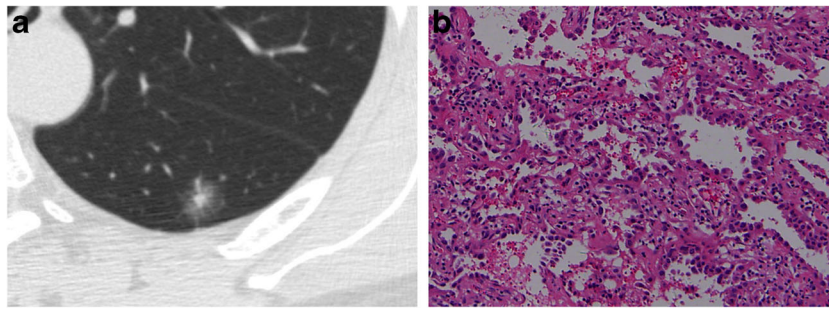


Fig. 4 A 48-year-old man with a MIA in the left lower lobe of the lung. Axial HRCT image showing a 14-mm diameter oval MGGN with a 3.8-mm diameter solid component, a CT value of -553 HU in the ground-

glass component and a CT value of -160 HU in the solid component (a). Photomicrograph of the resected specimen showing an acinar growth pattern (b, H & E, $\times 100$)

nodules involved multiple lobes in the remaining patient who underwent simultaneous lobectomy and wedge resection. Two patients exhibited pathological invasion of the visceral pleura, and no patients exhibited regional lymph node metastasis.

CT screening

CT scans were obtained with a 64-detector row scanner (Brilliance, Philips, USA) at the end of inspiration during a single breath hold. The routine CT scans were initially performed with a collimation of 64×0.625 mm and a FOV of 400 mm. When a lung nodule was identified, target HRCT was performed with the following parameters: collimation, 64×0.625 mm; pitch, 0.64; section thickness and interval, 1.0 and 1.0 mm, respectively; 1-3 second scan time; matrix, 1024×1024 ; FOV, 180 mm; 120 kVp; and 300 mA. The reconstruction algorithms for the routine and target HRCT scans were “standard” and “sharp”, respectively.

Evaluation of the HRCT features

The qualitative variables were assessed on the target HRCTs in the lung windows (width, 1450 HU; level, -520 HU) independently by two observers (Y.Z. and Y.S. who had 5 and 16 years of experience in chest imaging, respectively), and

discrepancies were resolved by consensus. The HRCT findings for each nodule were analysed according to the following parameters: (1) density (pure or mixed GGN, PGGN or MGGN); (2) lobulated shape; (3) spiculated margin; (4) air bronchogram; (5) abnormal vascular change (dilated, rigid, convergent or tortuous; single observations were recorded when multiple changes were observed. We traced the vessel from the nodule to the hilum to determine its source as pulmonary or bronchial, and determined whether it was an artery or vein); (6) bubble lucency (round or oval air attenuation inside the GGN that eliminated the air bronchogram); and (7) pleural indentation. The quantitative variables included the following: the CT values of the pure ground-glass and solid components of the GGN (assessed in the largest region of interest that excluded pulmonary vessels), and the diameters of the nodule and solid component (the largest diameters on the axial sections). The measurements were performed by a single radiologist (Y.Z.), repeated three times and averaged.

Pathological evaluation

The surgically resected nodules were histopathologically analysed and classified by two experienced lung pathologists by consensus according to the 2011 classification of lung adenocarcinomas.

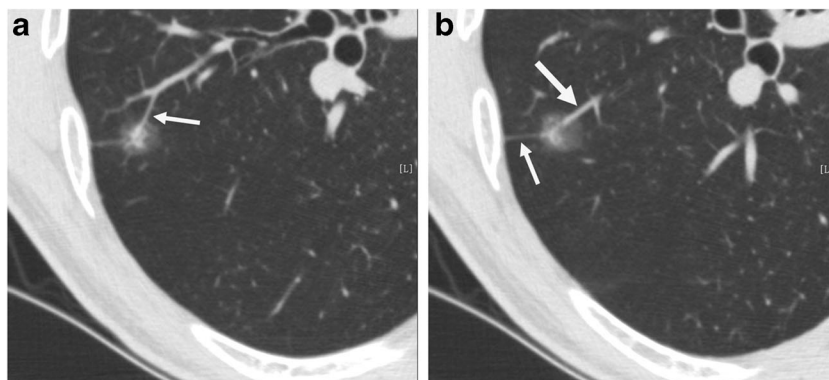


Fig. 5 A 56-year-old man with a lepidic predominant IAC with a papillary component in the right lower lobe of the lung. Axial HRCT images showing a MGGN of 13.6 mm in diameter with a 6.8-mm diameter solid

component, a rigid pulmonary vein (*thin arrow*) in the upper plane (a), a mildly dilated and rigid pulmonary artery (*thick arrow*) and a pleural indentation in the lower plane (*thin arrow*) (b)

Table 2 Multivariable logistic regression analysis of the AIS-MIA and IAC groups

Variables	Odds Ratio	95% Confidence Interval	P Value
Diameter of nodule	1.296	1.080–1.555	0.005
Diameter of solid component	1.181	1.005–1.387	0.044
CT value of ground glass component	1.004	1.000–1.009	0.054
CT value of solid component	1.005	1.000–1.010	0.037
Lobulated shape	1.099	0.342–3.537	0.874
Spiculated margin	0.997	0.171–5.825	0.998
Abnormal pulmonary vein	1.111	0.393–3.144	0.842
Abnormal pulmonary artery	1.457	0.556–3.817	0.443
Air bronchogram	2.841	1.047–7.711	0.040
Pleural indentation	0.579	0.209–1.603	0.293

Statistical analysis

The HRCT features of the two groups of lung nodules were compared. The quantitative variables were compared using two-sample Wilcoxon rank-sum tests, and the qualitative variables were compared with Pearson χ^2 tests. The variables that exhibited statistically significant differences were included in a multivariate logistic regression analysis. Receiver operating characteristic (ROC) analyses were conducted for the variables that exhibited statistically significant differences in the multivariate logistic regression. The cutoff values were defined as those for which the sensitivity plus specificity value was maximal. The interobserver agreements regarding the qualitative HRCT features were investigated using weighted κ statistics. *P* values < 0.05 were considered statistically significant. All statistical data were analysed using the SPSS 16.0 software program.

Results

The comparisons of the morphological features of the GGNs in AIS-MIAs with the IACs on HRCT are summarized in Table 1. Compared with the AIS-MIA group, the IACs exhibited larger nodule (15.2 mm vs. 11.1 mm, *p* = 0.000) and solid component diameters (10.3 mm vs. 6.1 mm, *p* = 0.000), higher CT values for the ground-glass components (-396 HU vs. -546 HU, *p* = 0.000) and solid components of the GGNs (-130 HU vs. -231 HU, *p* = 0.000) (Figs. 1, 2, 3 and 4), and greater frequencies of lobulated shape (*p* = 0.000),

spiculated margin (*p* = 0.009), abnormal pulmonary artery (*p* = 0.000), abnormal pulmonary vein (*p* = 0.000), air bronchogram (*p* = 0.000) and pleural indentation (*p* = 0.000) (Fig. 5). The results of the multivariate logistic regression analysis of the GGNs in the AIS-MIAs and IACs are illustrated in Table 2. This table indicates that larger nodule and solid component diameters, higher CT values of the solid components, and air bronchogram were significantly associated with the IACs (*p* = 0.005, 0.044, 0.037 and 0.040, respectively). The cutoffs and their diagnostic performances in distinguishing the AIS-MIA and IAC groups as determined by ROC analyses are summarized in Table 3 (Fig. 6). The cutoff nodule and solid component diameters were 12.2 mm (sensitivity: 85 %, specificity: 62 %) and 6.7 mm (sensitivity: 79 %, specificity: 62 %), respectively, and the cutoff CT value for the solid components was -192 HU (sensitivity: 77 %, specificity: 62 %).

The interobserver agreement results regarding the HRCT features of the GGNs are listed in Table 4. The κ values ranged from 0.645 to 0.977.

Discussion

Previous studies have found that PGGN does not necessarily indicate AIS and vice versa [11, 12]. Our study produced the similar results. We observed 58 AIS-MIAs appearing as MGGNs and seven IACs appearing as PGGNs. Additionally, the present study revealed that a larger nodule diameter was one factor that was independently associated with IAC at a

Table 3 The diagnostic performances of the cutoff values for the different variables in distinguishing the AIS-MIA and IAC groups

Variables	Cutoff value	Sensitivity	Specificity	AUC	95% confidence interval
Diameter of nodule	12.2 mm	85 %	62 %	0.75	0.66 ~ 0.83
Diameter of solid component	6.7 mm	79 %	62 %	0.79	0.72 ~ 0.86
CT value of solid component	-192 HU	77 %	62 %	0.74	0.66 ~ 0.82
Air bronchogram	—	—	—	0.64	0.54 ~ 0.73

AUC: the area under the curve

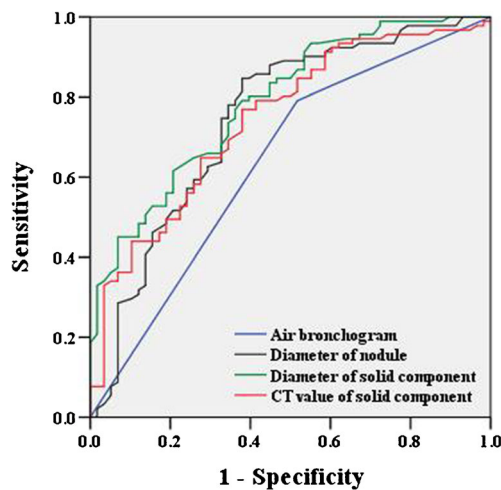


Fig. 6 Graph illustrating the ROC curves results for the variables found to be significant in the multivariate logistic regression. The areas under the curves for the nodule and solid component diameters, the CT value of the solid component, and the presence of an air bronchogram were 0.75, 0.79, 0.74, and 0.64, respectively

cutoff diameter of 12.2 mm, which yielded a sensitivity, specificity and area under the curve (AUC) of 85 %, 62 %, and 0.75, respectively. Kim et al. [12] found that the mean diameter of GGNs of lung adenocarcinomas with predominant BAC components is $13 \text{ mm} \pm 6.9$, and that of AAHs is $8 \text{ mm} \pm 3.8$. At a cutoff diameter of 10 mm for preinvasive PGGN lesions, a sensitivity of 53 % and a specificity of 100 % have been reported, and the cutoff diameter of 14 mm for MIA-IACs in MGGNs has been reported to yield a sensitivity of 67 % and a specificity of 74 % [13]. Moreover, a cutoff diameter of 11 mm for IACs in PGGNs has been reported to yield a sensitivity of 96 % and a specificity of 47 % [14], and a cutoff of 12.5 mm has been reported for MIA-IACs [15]. Because our study focused on differentiating AIS-MIAs and IACs, it is reasonable that the identified cutoff diameter differed from those of previous studies. However, the optimal cutoff value remains controversial.

The ROC curve revealed that the most powerful parameter for predicting IAC was the diameter of the solid component (6.7 mm), which yielded a sensitivity and specificity of 79 %

Table 4 Interobserver agreements for the CT features of the GGNs

Variables	Observer 1	Observer 2	k value
Density (PGGN/MGGN)	89/148	93/144	0.911
Lobulated shape	73	65	0.837
Spiculated margin	18	12	0.645
Abnormal pulmonary vein	128	117	0.739
Abnormal pulmonary artery	84	77	0.840
Air bronchogram	139	122	0.805
Bubble lucency	22	24	0.759
Pleural indentation	60	58	0.977

and 62 %, respectively with an AUC of 0.79. Cohen et al. [16] also concluded that the size of the solid component is the only factor that is independently associated with IAC in Caucasian patients. These authors reported a cutoff diameter of 9 mm for the solid component, which is larger than our cutoff value because larger nodules were observed in their study. There is a strong correlation between the diameter of the solid component on CT and the invasive component on pathology [17]. The solid component of a GGN usually represents the invasive portion of the tumour, collapsed alveolar space or fibrotic proliferation [18, 19].

Our study also revealed the mean CT values of the solid components were -231 HU for the AIS-MIAs and -130 HU for the IACs, and these values were significantly associated with IAC at the cutoff CT value of -192 HU. Our previous study revealed that the mean CT values of the solid components of GGNs of AAH-AISs and MIAs are -318 HU and -195 HU, respectively, and that this value was an independent differentiator of MIAs and AAH-AISs [11]. The odds ratio for the CT values of the ground-glass and solid components was not very high in our study; thus, further studies need to be performed.

Although GGNs with lobulated shape and spiculated margin were found to be significantly more frequent in the IACs in the univariate analyses, these factors were not significant in the multivariate analyses. These findings are inconsistent with those of previous studies that have investigated the HRCT features that differentiate IACs and pre-invasive lesions appearing as pulmonary GGNs and the features that differentiate malignant and benign pulmonary GGNs [13, 20]. Our purpose was to investigate the HRCT features that distinguish AIS-MIAs from IACs, which could explain the differences in the findings.

In our previous study [11], we found that abnormal pulmonary vein changes were more frequent in MIAs than pre-invasive lesions. However, in the current study, we found that pulmonary artery changes were more frequent in IACs than in AIS-MIAs. We infer that the walls of the pulmonary veins were thinner and less elastic and therefore more susceptible to shrinkage due to fibrosis compared with the arteries in the MIAs. With increases in invasiveness and angiogenesis and consequent increase in the blood supplies to the tumours, the differences between the AIS-MIA and IAC groups in abnormal pulmonary vein changes decreased, and the differences in the pulmonary artery changes increased [15, 21].

The relationships between solitary pulmonary nodules and bronchi have been described as abruptly obstructive, patent, tapered and narrowing and running around with an intact lumen [22]. Moreover, patent bronchi are more common in adenocarcinoma than squamous carcinoma patients [23]. Intratumoural bronchi were visualized in 37 % of nodules < 2 cm in the study by Cui et al. [23]. Yoshino et al. [24] indicated that an air bronchogram is a good independent prognostic factor. In contrast, our study found that this sign was associated with more invasive adenocarcinomas (34 % of the AIS-

MIA versus 78 % of the IACs). We infer that air bronchogram is associated with the shrinkage of intratumoural fibrosis, and that IACs are associated with more intratumoural fibrosis. Further studies are required to understand the relationship between air bronchogram and tumour invasiveness.

Pleural indentation on CT is not pathologically equivalent to pleural invasion [25, 26], but it is an independent predictor of poor prognoses [24]. Our study revealed that pleural indentation was more frequently associated with IAC than with AIS and MIA. We infer that this sign is also associated with intratumoural desmoplastic reactions.

Among the 128 patients with resected single AIS-MIA nodules, only 30 patients underwent segmentectomy or wedge resection. If HRCT can be used to confidently discriminate IACs from AISs and MIAs prior to surgery, segmental and wedge resection procedures can be conducted more frequently and benefit more patients. Therefore, our results will play an important role in the selection of the optimal surgical procedure.

This study had several limitations. First, only small numbers patients with IACs in PGGNs were enrolled. Second, because the nodules were small, some HRCT features, such as spiculated margin, were less typical, and inter-observer agreements were not perfect.

Conclusions

In conclusion, lung IACs appearing as GGNs frequently exhibited nodule and solid component diameters ≥ 12.2 mm and 6.7 mm, respectively, solid component CT values of -192 HU or greater, and an air bronchogram. Therefore, these GGNs cannot be candidates for sublobar resection. In contrast, GGNs that do not exhibit these characteristics are likely candidates for sublobar resection.

Acknowledgments The scientific guarantor of this publication is Jin Wei Qiang. The authors of this manuscript declare no relationships with any companies, whose products or services may be related to the subject matter of the article. This study has received funding by grants from national natural science foundation of China (81171340) and Science and Technology Commission of Shanghai (10411956800). One of the authors has significant statistical expertise. Institutional Review Board approval was obtained. Written informed consent was waived by the Institutional Review Board. Methodology: retrospective, diagnostic or prognostic study, performed at one institution.

References

- Nakata M, Saeki H, Takata I et al (2002) Focal ground-glass opacity detected by low-dose helical CT. *Chest* 121:1464–1467
- Travis WD, Brambilla E, Noguchi M et al (2011) International association for the study of lung cancer/American thoracic society/European respiratory society international multidisciplinary classification of lung adenocarcinoma. *J Thorac Oncol* 6:244–285
- Zhang J, Wu J, Tan Q, Zhu L, Gao W (2013) Why do pathological stage IA lung adenocarcinomas vary from prognosis? A clinicopathologic study of 176 patients with pathological stage IA lung adenocarcinoma based on the IASLC/ATS/ERS classification. *J Thorac Oncol* 8:1196–1202
- Van Schil PE, Asamura H, Rusch VW et al (2012) Surgical implications of the new IASLC/ATS/ERS adenocarcinoma classification. *Eur Respir J* 39:478–486
- Tsutani Y, Miyata Y, Nakayama H et al (2014) Appropriate sublobar resection choice for ground glass opacity-dominant clinical stage IA lung adenocarcinoma wedge resection or segmentectomy. *Chest* 145:66–71
- El-Sherif A, Gooding WE, Santos R et al (2006) Outcomes of sublobar resection versus lobectomy for stage I non-small cell lung cancer: A 13-year analysis. *Ann Thorac Surg* 82:408–416
- Altorki NK, Yip R, Hanaoka T et al (2014) Sublobar resection is equivalent to lobectomy for clinical stage IA lung cancer in solid nodules. *J Thorac Cardiovasc Surg* 147:754–762
- Donahue JM, Morse CR, Wigle DA et al (2012) Oncologic efficacy of anatomic segmentectomy in stage IA lung cancer patients with T1a tumors. *Ann Thorac Surg* 2012(93):381–388
- Nomori H, Iwatani K, Kobayashi H, Mori A, Yoshioka S (2006) Omission of mediastinal lymph node dissection in lung cancer: its techniques and diagnostic procedures. *Ann Thorac Cardiovasc Surg* 12:83–88
- Nakahara R, Yokose T, Nagai K, Nishiwaki Y, Ochiai A (2001) Atypical adenomatous hyperplasia of the lung: a clinicopathological study of 118 cases including cases with multiple atypical adenomatous hyperplasia. *Thorax* 56:302–305
- Zhang Y, Qiang JW, Ye JD, Ye XD, Zhang J (2014) High resolution CT in differentiating minimally invasive component in early lung adenocarcinoma. *Lung Cancer* 84:236–241
- Kim HY, Shim YM, Lee KS, Han J, Yi CA, Kim YK (2007) Persistent pulmonary nodular ground-glass opacity at thin-section CT: histopathologic comparisons. *Radiology* 245:267–275
- Lee SM, Park CM, Goo JM, Lee HJ, Wi JY, Kang CH (2013) Invasive pulmonary adenocarcinomas versus preinvasive lesions appearing as ground-glass nodules: differentiation by using CT features. *Radiology* 268:265–273
- Eguchi T, Yoshizawa A, Kawakami S et al (2014) Tumor size and computed tomography attenuation of pulmonary pure ground-glass nodules are useful for predicting pathological invasiveness. *PLoS ONE* 9:e97867
- Liu LH, Liu M, Wei R et al (2015) CT findings of persistent pure ground glass opacity: can we predict the invasiveness? *Asian Pac J Cancer Prev* 16:1925–1928
- Cohen JG, Reymond E, Lederlin M et al (2015) Differentiating pre- and minimally invasive from invasive adenocarcinoma using CT-features in persistent pulmonary part-solid nodules in Caucasian patients. *Eur J Radiol* 84:738–744
- Lee HK, Goo JM, Park SJ et al (2014) Correlation between the size of the solid component on thin-section CT and the invasive component on pathology in small lung adenocarcinomas manifesting as ground-glass nodules. *J Thorac Oncol* 9:74–82
- Noguchi M, Morikawa A, Kawasaki M et al (1995) Small adenocarcinoma of the lung - histologic characteristics and prognosis. *Cancer* 75:2844–2852
- Park CM, Goo JM, Lee HJ, Lee CH, Chun EJ, Im JG (2007) Nodular ground-glass opacity at thin-section CT: histologic correlation and evaluation of change at follow up. *RadioGraphics* 27:391–408
- Lee HJ, Goo JM, Lee CH et al (2009) Predictive CT findings of malignancy in ground-glass nodules on thin-section

- chest CT: the effects on radiologist performance. *Eur Radiol* 19:552–560
21. Gao F, Li M, Ge XJ et al (2013) Multi-detector spiral CT study of the relationships between pulmonary ground-glass nodules and blood vessels. *Eur Radiol* 23:3271–3277
 22. Qiang JW, Zhou KR, Lu G et al (2004) The relationship between solitary pulmonary nodule and bronchus: MSCT-pathologic correlation. *Clin Radiol* 59:1121–1127
 23. Cui Y, Ma DQ, Liu WH (2009) Value of multiplanar reconstruction in MSCT in demonstrating the relationship between solitary pulmonary nodule and bronchus. *Clin Imaging* 33: 15–21
 24. Yoshino I, Nakanishi R, Kodate M et al (2000) Pleural retraction and intra-tumoral air-bronchogram as prognostic factors for stage I pulmonary adenocarcinoma following complete resection. *Int Surg* 85:105–112
 25. Yamazaki K, Yoshino I, Yohena T et al (2007) Clinically predictive factors of pathologic upstaging in patients with peripherally located clinical stage IA non-small cell lung cancer. *Lung Cancer* 55:365–369
 26. Ikehara M, Saito H, Kondo T et al (2012) Comparison of thin-section CT and pathological findings in small solid-density type pulmonary adenocarcinoma: prognostic factors from CT findings. *Eur J Radiol* 81:189–194